A comparison of single shot nanosecond and femtosecond polarization-resolved laser-induced breakdown spectroscopy of Al*

Nakimana Agnes, Tao Hai-Yan(陶海岩), Hao Zuo-Qiang(郝作强), Sun Chang-Kai(孙长凯), Gao Xun(高 勋), and Lin Jing-Quan(林景全)†

School of Science, Changchun University of Science and Technology, Changchun 130022, *China*

(Received 21 May 2012; revised manuscript received 18 June 2012)

Aluminum samples have been analyzed by femtosecond polarization-resolved laser-induced breakdown spectroscopy (fs-PRLIBS). We compare the obtained spectra with those obtained from nanosecond PRLIBS (ns-PRLIBS). The main specific features of fs-PRLIBS are that a lower plasma temperature leads to a low level of continuum and no species are detected from the ambient gas. Furthermore, signals obtained by fs-PRLIBS show a higher stability than those of ns-PRLIBS. However, more elements are detected in the ns-PRLIBS spectra.

Keywords: polarization-resolved laser-induced breakdown spectroscopy, femtosecond laser, nanosecond laser, shielding

PACS: 42.62.Fi, 52.38.Mf, 78.47.J– **DOI:** 10.1088/1674-1056/22/1/014209

1. Introduction

Laser-induced breakdown spectroscopy (LIBS) is a powerful elemental analysis technology based on the optical emission spectra of plasma produced by the interaction of a high-power laser with gas, liquid and solid media. The increasing popularity of this technique is due to its simplicity in experimental set up and wide flexibility in investigating materials, which needs little or no pre-treatment of the sample before analysis. The tasks of using LIBS are the detection of metal contents in alloys,[1–3] trace detection of metal elements in soils for environmental pollution analysis,[4–6] on-line control of industrial processes,[7] fast characterization of material in archeological objects and works of art,[8,9] and many others.

The LIBS technique is based on the analysis of lines emitted from a laser-induced plasma, which is obtained by focusing a pulsed laser beam onto a sample. In the sample, elements are atomized, ionized and excited at high temperatures provided by the laser beam. When the nuclei/ions and electrons recombine and further relax to low-lying states, light of characteristic wavelengths is emitted. Due to the fact that all elements emit light of characteristic frequencies when they are sufficiently excited, LIBS can in principle detect all elements.

The mechanisms responsible for material removal by laser beam are thermal melting and evaporation, or some kind of explosive evaporation depending on laser light fluence and its pulse duration.[10] If the laser ablation threshold is reached, plasma is ignited, heated, and sustained due to the inverse Bremsstrahlung absorption of the laser photons.[11] The typical characteristic time scales of different processes involved are free electron heating and thermalization that takes approximately 100 fs; hot electron gas cooling and considerable energy transfer to the lattice, which last a few picoseconds; thermal diffusion in the bulk, which takes place on a time scale of 10 ps; and the onset of thermal melting and ablation that occurs after 100 ps.[12] Thus, a laser light with a pulse duration longer or shorter than a few picoseconds does not have the same effect on the target and on the formed plasma. A laser light with pulse duration longer than a few picoseconds does not interact the whole time with the original thermodynamic state of the material. Instead, it interacts with different transient states, and with the plasma of evaporated material and the buffer gas close to the sample surface. The majority of material removed in the process is evaporated from molten metal, and the preferential volatilization of different elements with different melting temperatures occurs.[13,14] However, a laser beam with pulse duration of 100 fs or shorter interacts only with the electron sub-system of a material. Before the material undergoes any change in the thermodynamic state, the laser pulse is over, and most of the energy is deposited into the sample. Material removal occurs after the laser pulse.[15] The differences in plasma formation and evolution due to the pulse duration determine the properties of the radiation emitted from the plasma.

So far, many studies have investigated the influence of pulse duration on the LIBS results. Chichkov *et al.* demonstrated that the femtosecond regime was better than the picosecond and nanosecond ones for precise material processing.[16] Margetic *et al.* observed a lower ablation threshold for the femtosecond regime than the nanosecond one.[17] Le Drogoff *et al.* showed that the femtosecond and

*Project supported by the National Natural Science Foundation of China (Grant Nos. 11211120156, 11274053, 11074027, 61178022, and 60978014), the Science and Technology Department of Jilin Province, China (Grant Nos. 20100521, 20100168, and 20111812), and the SRF for ROCS, SEM.

†Corresponding author. E-mail: linjingquan@cust.edu.cn

© 2013 Chinese Physical Society and IOP Publishing Ltd

nanosecond regimes have the same limit of detection.[18] Eland *et al.* presented the advantages, such as the high precision of sample ablation, lower continuum background, and faster plasma dissipation, of the picosecond and femtosecond regimes compared with the nanosecond one.[19] Sirven *et al.* used the time-resolved spectra obtained with a nanosecond and femtosecond laser to analyze the continuum emission, and the atomic and ionic spectral lines of aluminum.[20] They concluded that the temporal behaviors of the continuum and the spectral lines depend much more on the laser fluence than on the pulse duration. Liu *et al.* reported a single shot femtosecond and nanosecond PRLIBS with different fluencies.[21] They observed that the signal to background (S/B) ratio, the resolution and the detection limit of PRLIBS were improved with respect to a conventional LIBS.

In this paper, we report a comparison study of the nanosecond and femtosecond polarization resolved laser-induced breakdown spectroscopy (ns-PRLIBS and fs-PRLIBS) spectra obtained using the same laser fluence. The experiment is performed on a metallic aluminum sample at a fluence of 20 J/cm^2. A Glan–Thompson polarizer is used to filter out the background. We first analyze the polarization effect on the ns-LIBS and fs-LIBS signals. Then, the signals obtained without use of the polarizer are compared with those obtained by using a polarizer, which is oriented at its minimum transmission angle. Furthermore, we analyze in detail the ns-PRLIBS and fs-PRLIBS spectra and give explanations on the differences between them.

2. Experimental set-up

The schematic diagram of our experimental set-up is shown in Fig. 1. Two kinds of lasers are used: a nanosecond Nd: YAG laser operating with a pulse duration of 10 ns, repetition rate of 10 Hz, and a wavelength of 1064 nm; and a femtosecond Ti:Sa amplifier operating with a pulse duration of 100 fs, repetition rate of 10 Hz, and wavelength of 800 nm. The pulse energy used is 3.5 mJ in the nanosecond case while it is 0.8 mJ in the femtosecond case. At the output of the laser, the beams initially have the same size ($\sim$ 8 mm of diameter). The laser beam is focused through a lens L_1($f = 200$ mm) on the aluminum alloy in air. The focusing geometry is changed and optimized by the precise translation of the lens with a micrometer screw. The laser spot diameter is about 100 μm at the focal point when a femtosecond laser is used while it is about 150 μm by using a nanosecond laser. Our sample is Al 2024 (YL 12),, and consisted of Al ($\sim$ 91%), Si ($<$ 0.5%), Fe ($<$ 0.5%), Cu (3.8%–4.9%), Mn (0.3%), Mg (1.2%–1.8%), Cr (0.1%), Zn (0.25%), Ti (0.15%), and others (0.05%). A two-dimensional translation stage (C-863 DC Motor controller) is used to make each laser pulse fall on a fresh target surface. The radiation emitted by a plasma plume is collected into an optical fiber by a pair of lenses L_2 ($f = 75$ mm) and L_3 ($f = 35$ mm). A filter behind lens L_2 is used to reduce the laser light reflection intensity in the plasma and to eliminate possible influence from the fundamental laser light. To measure the polarization of the plasma emission, a Glan–Thompson polarizer P is placed between the lens L_2 and L_3 at the focal point of L_2. The emission from the plume is recorded by a detection system (Ocean Optics USB 4000) in conjunction with an optical fiber. During the experiment, the incident direction of the laser beam was normal to the sample surface and the detection angle was at 60° from the normal direction of the sample surface. An integration time of 100 ms was used.

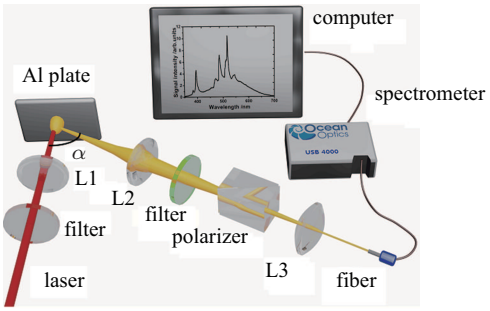


Fig. 1. (color online) Schematic diagram of the experimental set-up.

To investigate the plasma polarization, the spectrum intensity is measured by rotating the polarizer about its axis with an increment of 20°. The polarization degree is then calculated by

$$P = (I_{\max} - I_{\min}) / (I_{\max} + I_{\min}). \quad (1)$$

Here, $I_{\max}$ and $I_{\min}$ are chosen among all measurements. The polarization spectrum is then obtained by plotting P as a function of wavelength.

3. Results and discussion

Figure 2 shows the spectra for an Al target obtained with nanosecond (Fig. 2(a)) and femtosecond lasers (Fig. 2(b)), respectively. The solid curves correspond to the spectra obtained without the use of a polarizer (i.e., LIBS) while the dash-dot curves represent the spectra obtained by using a Glan–Thompson polarizer at its minimum transmission angle (i.e., PRLIBS). It is obvious that, in both cases, without the use of the polarizer, the spectrum is dominated by the continuum emission (solid curves). However, by using a polarizer oriented at its minimum transmission angle, the spectral intensity is reduced, which reveals more atomic and ionic lines (dash-dot curves). As a consequence, the signal to noise (S/N) and S/B ratios of the lines are improved. The S/N and S/B ratios are comparatively listed in Table 1. In each case, the lines of 517.26 nm and 588.38 nm are used to calculate the S/N and S/B ratios. From Table 1, the S/N ratio improvement due to

the use of polarizer at its minimum transmission angle is ∼1.2 times in ns-LIBS, while in fs-LIBS it is ∼ 3 times. The S/B ratio improvement for the line at 517.26 nm is ∼ 2 times in ns-PRLIBS while it is ∼ 3 times in fs-PRLIBS.

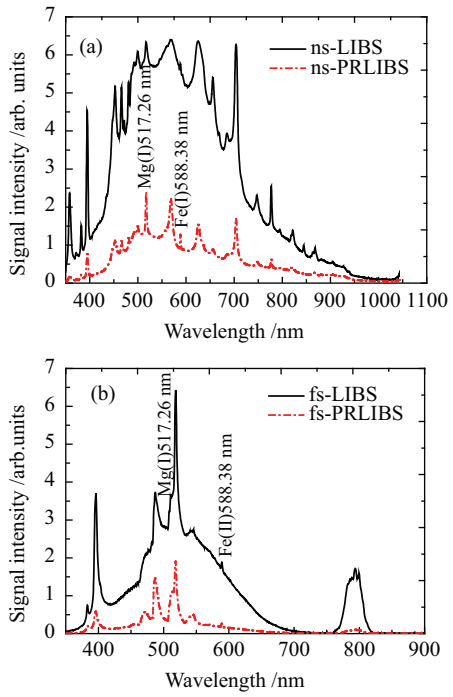


Fig. 2. (color online) Plasma emission spectra of Al produced by (a) Nd: YAG laser pulsed at 10 ns, with a fluence of 19.8 J/cm^2, and (b) Ti: Sapphire laser pulses at 100 fs, with a fluence of 20.3 J/cm^2. LIBS spectra (solid curve) and PRLIBS spectra (dash-dotted curve).

Table 1. Signal to noise (S/N) and signal to background (S/B) ratio.

	Lines/nm	S/N ratio in LIBS	S/N ratio in PRLIBS	S/B ratio in LIBS	S/B ratio in PRLIBS
ns	517.26	55.03	67.13	1.11	1.95
	588.38	6.44	7.24	1.03	1.46
fs	517.26	87.5	235.78	2.46	6.37
	588.38	12.73	35.54	1.25	1.67

Figure 3 shows the PRLIBS spectra produced with nanosecond (solid curve) and femtosecond (dash-dotted curve) laser irradiation. Some lines are observed in both regimes, while others are only observed in one regime and are absent in the other. Figure 3(a) shows that more lines are well resolved in ns-PRLIBS than those in fs-PRLIBS. Our result is similar to some previous observations.[20,21] For example, as shown in detailed spectra (Figs. 3(b)–3(e)), Al (II) lines are only observed in ns-PRLIBS. The fact that more elements can be detected in ns-PRLIBS than that in fs-PRLIBS should be attributed to the shielding effect. In ns-PRLIBS, when the plasma is formed, it continues to absorb the rest energy of the laser pulse, which results in a higher excited state and ions, e.g., the species (neutral or ionic) in the plasma can be excited (Fe I) or ionized (Al II). The situation is different in fs-PRLIBS. During the very first nanoseconds after the laser pulse, the plasma contains many ionic species. Due to the fact that there is no further interaction between the laser pulse and the plasma, the ionic species recombine rapidly in neutral and thus their intensities decrease.[20]

It is interesting to note that some species from the ambient air such as O (I) and N (II) are detected in ns-PRLIBS while they are absent in fs-PRLIBS. Our result agrees with the findings in the literature.[22] In the ns-PRLIBS case, the species (N_2, O_2) contained in air can be excited (O I) or ionized (N II) due to the interaction of a ns laser pulse with the air plasma. In contrast, there is no interaction between the plasma and laser pulse in fs-PRLIBS due to the shorter pulse duration.[12] The ablated material expands into a cold buffer gas. This can explain why these lines are absent in fs-PRLIBS.

It can also be noted from Fig. 3(a) that the continuum emission in ns-PRLIBS is greater than that in fs-PRLIBS. The contribution of the continuum emission can be clearly seen by comparing the S/B ratio in the last column of Table 1. For example, the S/B ratio for 517.26 nm in fs-PRLIBS is about 4 times higher than that in ns-PRLIBS. To understand why the continuum emission is higher in ns-PRLIBS, we calculate the plasma temperature by assuming the plasma is in a local thermodynamic equilibrium (LTE). In the case of fs-PRLIBS, few lines are observed and therefore it is not possible to use the Boltzmann plot method. Thus, the two line method is used to calculate the temperature[23]

$$\frac{I_1}{I_2} = \frac{A_1 g_1 \lambda_2}{A_2 g_2 \lambda_1} \exp\left(-\frac{E_1 - E_2}{k_B T_e}\right). \quad (2)$$

Here, A is the transition probability, g the statistical weight, λ the wavelength, E the excited level energy, k_B the Boltzmann constant, T_e the electron temperature and the subscripts 1 and 2 refer to two spectral lines of the same element. The lines Mg (I) 382.93 nm and Mg (I) 517.26 nm are used. The values of A, g and E can be found in NIST database.[24] The plasma temperature calculated in fs-PRLIBS is of 2596 K while it is of 5346 K in the case of ns-PRLIBS. The ns-plasma temperature is 2 times higher than that of an fs-plasma. Since it is known that the continuum emission is decisively related to the plasma temperature ($\propto T^4$),[22] the higher plasma temperature for the case of ns-PRLIBS explains why the continuum is higher in ns-PRLIBS than in fs-PRLIBS.

Plasma polarization spectra in ns-LIBS and fs-LIBS are given in Fig. 4. The polarizer axis is rotated by an increment of 20° each time the signal is recorded. The polarization spectrum is then obtained by plotting the polarization degree P as a function of wavelength. A comparison of the emission spectrum (dash-doted curve) and the polarization spectrum (solid curve) shows that, in ns-PRLIBS (Fig. 4(a)) as in fs-PRLIBS (Fig. 4(b)), the discrete lines appear as dips

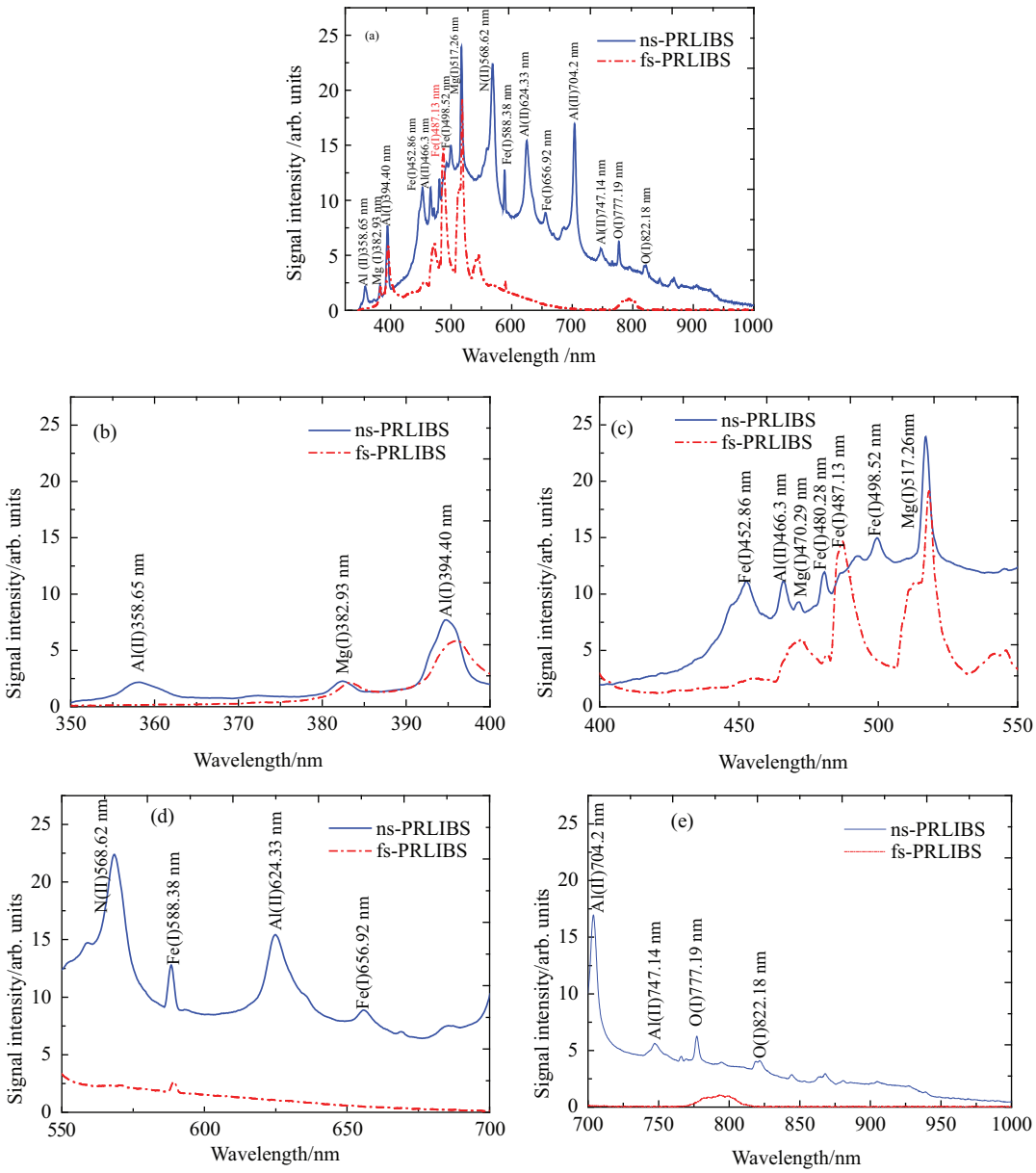


Fig. 3. (color online) Plasma emission spectra of Al produced by ns (solid curve) and fs (dash-dotted curve) with a fluence of 20 J/cm^2: Overview (a) and detailed (b – e) spectra of ns-PRLIBS and fs-PRLIBS.

in the polarization spectra, which indicate that the continuum is much more polarized than the discrete line emissions. In both cases, the continuum polarization degree at some wavelengths is higher than 80%. A comparison of fs-PRLIBS and ns-PRLIBS polarization spectra shows that the polarization degree of the lines in fs-PRLIBS is smaller and has a higher S/B ratio than that in ns-PRILIBS. A higher polarization characteristic of the continuum component is the reason why the polarizer oriented at its minimum transmission angle can reduce the continuum while the discrete lines are still present.

Signal stability of spectra in the cases of ns-PRLIBS and fs-PRLIBs is also compared. It is found that fs-PRLIBS shows a higher signal stability than that of ns-PRLIBS. To calculate the relative standard deviation (RSD), four spectra were used. The integration time was fixed to be 100 ms and no accumulation of spectra was done. The relative standard deviation of line Fe I at 588.38 nm is used for comparison. The RSD of the line is 11.7% for ns-PRLIBS while it is only 2.3% for the fs-PRLIBS. The RSD of the fs-PRLIBS spectrum is much lower, i.e., with higher stability, than that obtained in ns-PRLIBS. The difference is due to their plasma creation mechanisms. In fs-PRLIBS, the plasma creation is mainly due to the multiphoton ionization,[25] while in ns-PRLIBS, it is mainly due to the cascade ionization (avalanche).[26] Experimentally, it is found that the delay between the beginning of a long pulse and the initiation of the avalanche is about 3 ns.[27] During that period, the amount of energy absorbed from the pulse fluctuates and this fluctuation reduces the plasma stability.[28] However, in the multiphton ionization regime, each ion is created directly by the laser and each ion creation is an independent event. That can explain why fs-PRLIBS is more stable.

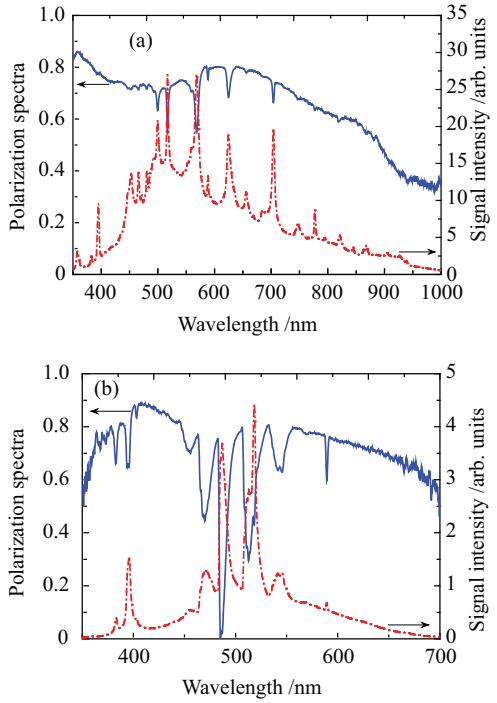


Fig. 4. (color online) Plasma emission spectra (dash-dotted curve) and plasma polarization spectrum (solid curve) of Al produced by (a) Nd: YAG laser pulsed at 10 ns, with a fluence of 19.5 J/cm^2 and (b) Ti: Sapphire laser pulses at 100 fs, with a fluence of 20.3 J/cm^2.

4. Conclusion

In this paper, we first compare the LIBS and PRLIBS measurements obtained in single shot experiments by using nanosecond and femtosecond laser pulses with an excitation fluence of 20 J/cm^2. It is shown that in both cases, the LIBS spectrum is dominated by a continuum emission while the continuum is largely attenuated in PRLIBS. It is also shown that the continuum has a higher polarization degree ($> 80\%$ at some wavelengths) than that of discrete lines. A comparison between fs and ns-PRLIBS demonstrates attractive features related to the use of ultrashort pulses in the LIBS analysis. The fs-PRLIBS spectra show a low level of continuum and less interference with emissions from the ambient air. These attractive features are related to the lower temperature of the femtosecond laser-induced plasma. In addition, the fs-PRLIBS signals possess a higher stability than those of ns-PRLIBS, instead, the ns-PRLIBS spectrum provides a higher sensibility.

Acknowledgements

The authors wish to thank Mostafa Alshershaby and Acner Camino Benech for their helpful discussion.

References

[1] Bleiner D, Bogaerts A, Belloni F and Nassisi V 2007 *J. Appl. Phys.* **101** 083301
[2] Tawfik W 2007 *Progress in Physics* **2** 42
[3] Baudelet M, Willis C, Shah L and Richardson M 2010 *Opt. Express* **18** 7905
[4] Tawfik W and Askar A 2007 *Progress in Physics* **1** 46
[5] Yang N F 2009 *Elemental Analysis of Soils Using Laser-Induced Breakdown Spectroscopy* (LIBS) (Master's Thesis) (Knoxville : University of Tennessee)
[6] Xie C, Lu J, Li P, Li J and Lin Z 2009 *Opt. Lett.* **7** 545
[7] Bol'shakov A A, YooJ H, Liu C, Plumer J R and Russo R E 2010 *Appl. Opt.* **49** C132
[8] Alvira F C, Ramirez Rozzi F and Bilmes G M 2010 *Appl. Spectrosc.* **64** 313
[9] Galiova M, Kaiser J, Fortes F, Novotny K, Malina R, Prokes L, Hrdlicka A, Vaculovic T, Fisakova M N, Svoboda J, Kanicky V and Laserna J J 2010 *Appl. Opt.* **49** C191
[10] Miotello A and Kelly R 1999 *Appl. Phys.* A **69** 67
[11] Russo R E 1995 *Appl. Spectrosc.* **49** 14A
[12] von der Linder D, Sokolowski-Tinten K and Bialkowski J 1997 *Appl. Surf. Sci.* **109/110** 1
[13] Baldwin J 1970 *Appl. Spectrosc.* **24** 429
[14] Cromwell E and Arrowsmith P 1995 *Appl. Spectrosc.* **49** 1652
[15] Leitz K H, Redlingshofer B, REG Y, Otto A and Schmidt M 2011 *Physics Procedia* **12** 230
[16] Chichkov B N, Momma C, Nolte S, von Alvensleben F, Tunnermann A 1996 *Appl. Phys. A* **63** 109
[17] Margetic V, Pakulev A, Stockhaus A, Bolshov M, Niemax K and Hergenroder R 2000 *Spectrochim. Acta* (Part B) **55** 1771
[18] Le Drogoff B, Margot J, Chaker M, Sabsabi M, Barhelemy O and Johnston T W, Laville S, Vidal F and von Kaenel Y http://dx.doi.org/10.1016/S0584-8547(01)00187-22001 *Spectrochim. Acta* (Part B) **56** 987
[19] Eland K L, Stratis D N, Gold D M, Goode S R and Angel S M 2001 *Appl. Spectrosc.* **55** 286
[20] Sirven J B, Bousquet B, Canoini L and Sarger L 2004 *Spectrochimica Acta* (Part B) **59** 1033
[21] Liu Y, Penczak J S and Gordon R J 2010 *Opt. Lett.* **35** 112
[22] Baudelet M, Guyon L, Yu J and Wolf J P 2006 *J. Appl. Phys.* **99** 084701
[23] Amoruso S, Bruzzese R, Spinelli N and Velotta R 1999 *J. Phys.* B: *At. Mol. Opt. Phys.* **32** R131.
[24] http://physics.nist.gov/PhysRefData/ASD/lines_form.html.
[25] Wu J, Zeng J and Guo C 2006 *Phys. Rew. Lett.* **96** 243002
[26] Zhao Y, Liang Y, Zhang N, Wang M and Zhu X 2008 *Opt. Lett.* **33** 2467
[27] Shverdin M Y, Goda S N, Yin G Y and Harris S E 2006 *Opt. Lett.* **31** 1331
[28] Heins A M and Guo C L 2012 *Opt. Lett.* **37** 599